LASCO OBSERVATIONS OF DISCONNECTED MAGNETIC STRUCTURES OUT TO BEYOND 28 SOLAR RADII DURING CORONAL MASS EJECTIONS

G. M. SIMNETT, S. J. TAPPIN, S. P. PLUNKETT, D. K. BEDFORD and C. J. EYLES

School of Physics and Space Research, University of Birmingham, B15 2TT, U.K.

O. C. ST. CYR, R. A. HOWARD, G. E. BRUECKNER, D. J. MICHELS, J. D. MOSES, D. SOCKER, K. P. DERE, C. M. KORENDYKE, S. E. PASWATERS and D. WANG

E.O. Hulbert Center for Space Research, Naval Research Laboratory, Washington, D.C. 20375–5320, U.S.A.

R. SCHWENN

Max-Planck-Institut für Aeronomie, Katlenburg-Lindau, Germany

P. LAMY, A. LLEBARIA and M. V. BOUT

Laboratoire d'Astronomie Spatiale, Marseille, 13376, France

Abstract. Two coronal mass ejections have been well observed by the LASCO coronagraphs to move out into the interplanetary medium as disconnected plasmoids. The first, on July 28, 1996, left the Sun above the west limb around 18:00 UT. As it moved out, a bright V-shaped structure was visible in the C2 coronagraph which moved into the field-of-view of C3 and could be observed out to beyond 28 solar radii. The derived average velocity in the plane of the sky was 110 ± 5 km s^{-1} out to 5 solar radii, and above 15 solar radii the velocity was 269 ± 10 km s^{-1}. Thus there is evidence of some acceleration around 6 solar radii. The second event occurred on November 5, 1996 and left the west limb around 04:00 UT. The event had an average velocity in the plane of the sky of ~ 54 km s^{-1} below 4 $R_\odot$, and it accelerated rapidly around 5 $R_\odot$ up to 310 ± 10 km s^{-1}. In both events the rising plasmoid is connected back to the Sun by a straight, bright ray, which is probably a signature of a neutral sheet. In the November event there is evidence for multiple plasmoid ejections. The acceleration of the plasmoids around a projected altitude of 5 solar radii is probably a manifestation of the source surface of the solar wind.

1. Introduction

One of the essential requisites of solar coronal mass ejections is that they should not carry a significant net magnetic flux into the heliosphere. Not only is this not observed in the interplanetary medium, but it is clear that within the lifetime of the Sun, a steady state must have been established, within which current transient activity must fit. Therefore there must be a significant number of coronal mass ejections (CMEs) which disconnect from the Sun and propagate out as detached plasmoids. Such events so far have been difficult to detect, either from eclipse observations or from spaceborne coronagraphs over the last two decades. The first report of a disconnection event was by Illing and Hundhausen (1983) who interpreted observations from the Solar Maximum Mission (SMM). Webb and Cliver (1995) made a systematic search of both eclipse data and spaceborne coronagraph data up to
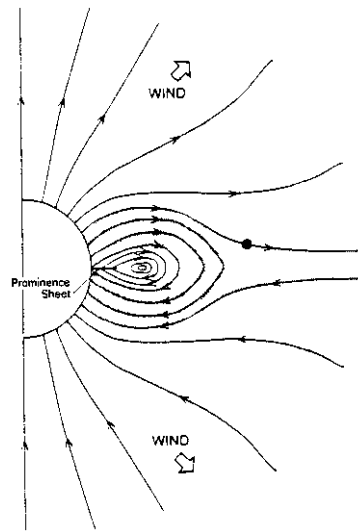
Figure 1. A model of the magnetic topology in a helmet streamer overlying a prominence. The lines of force in the high equatorial region enclose the equatorial interplanetary current sheet. Regions of high density are shaded. The closed magnetic field in the low-density cavity is normally in static equilibrium. The vertical prominence sheet is shown as a line extending out into the low density cavity. In this model the length runs in the azimuthal direction. (After Low, 1994.)

1980 for disconnection events. Although the data are not ideal for such a study, they nevertheless concluded that possibly over 10% of CMEs have disconnection features. St. Cyr and Burkepile (1990) suggested that this feature was only present in possibly 3% of all events.

McComas *et al.* (1989) had proposed a solution to the dilemma through the balancing of the newly-opened magnetic flux in CMEs via reconnection across the current sheet which extends above structures such as coronal helmet streamers. This would serve to detach a 'U'-shaped structure out into the corona. McComas *et al.* (1991) and McComas *et al.* (1992) presented observations of such events detected by SMM on July 27, 1988 and June 1 1989, respectively. However, their data were limited to the coronal region from 1.5 to $\gtrsim 5 \ R_\odot$.

Low (1996) has reviewed the theoretical modelling for such events. In an ideal situation, the closed field regions in the corona may be thought of as a high density helmet dome, with a streamer emerging from the top, representing the neutral sheet extending into interplanetary space. Frequently there will be a prominence in the low corona, with a low density 'cavity' above it. Figure 1 (reproduced from Low (1994)) shows a schematic of this situation. In the data we present here there is evidence for the disconnection and ejection from the Sun of structures virtually identical to that depicted in Figure 1. Thus we have convincing evidence that not only do disconnection events occur, but they occur in a manner predicted by theory.

2. The Observations

The observations we report here were taken with the set of three nested coronagraphs (LASCO) on the Solar and Heliospheric Observatory (SOHO) in 1996. A full description of LASCO may be found in Brueckner *et al.* (1995). They cover the corona in three concentric bands, from 1.1–3.0 (C1), 1.5–6.0 (C2), and 3.7–30 (C3) $R_\odot$. The images we present in this paper (with one exception) are from the C2 and C3 coronagraphs; they are responding to photospheric light which is Thomson-scattered off free electrons in the corona. Therefore the intensity reflects excess mass in the corona, and does not indicate temperature. The C1 coronagraph contains a scanning Fabry–Pérot interferometer and for the November 5 event the onset of the CME was observed in the line of Fe X. The two disconnection events originated near the west limb of the Sun and the estimated onset times were ∼18:00 UT on July 28 and ∼ 04:00 UT on November 5. There were no active regions near the west limb on either occasion and we know of no chromospheric response to the ejections.

2.1. THE JULY 28–29 EVENT

From the beginning of July 28, the equatorial streamer off the west limb gradually brightened. At the same time it swelled such that by 15:04 UT it was apparent that an eruption of some sort was probable. The C2 images showing this are presented in Figure 2.

The eruption first became visible in the C2 coronagraph at 18:56 UT when a bright feature appeared at ∼2 $R_\odot$ about 5° below the equator. This rapidly expanded outwards and some sample images from C2 are shown in Figure 3. Note that the original bright equatorial streamer is still visible just to the north of the equator off the west limb. At 22:02 UT on July 28 the ejected mass appears pear-shaped and is embedded within the expanded helmet streamer. By 00:00 UT it has moved outwards, leaving behind a bright strip connecting back to the Sun, with a darker region to the north. In the image at 01:19 UT on July 29, some thin bright lines are just visible on the northern edge of the dark region. These are seen better in the image at 02:37 UT, which has had the contrast enhanced to increase their visibility. The thin bright line bifurcates at around 3 $R_\odot$ in this image, and the lines are reproduced in white in the upper part of the frame to aid the eye. The trailing edge of the ejected mass is just visible to the right of the frame.

The evolution of the ejection is now seen best in the C3 coronagraph. Four partial frames are shown in Figure 4, taken at 03:39, 04:08, 04:48, and 06:06 UT, respectively. These images are difference images, and each has had the pre-event coronal image subtracted from it. This emphasises transient behaviour, but can clearly produce artefacts if long-lived features such as coronal streamers move through the field of view due to solar rotation. The ejection now begins to look like a bright bubble on a stem, with the brightest feature very close to the top of the
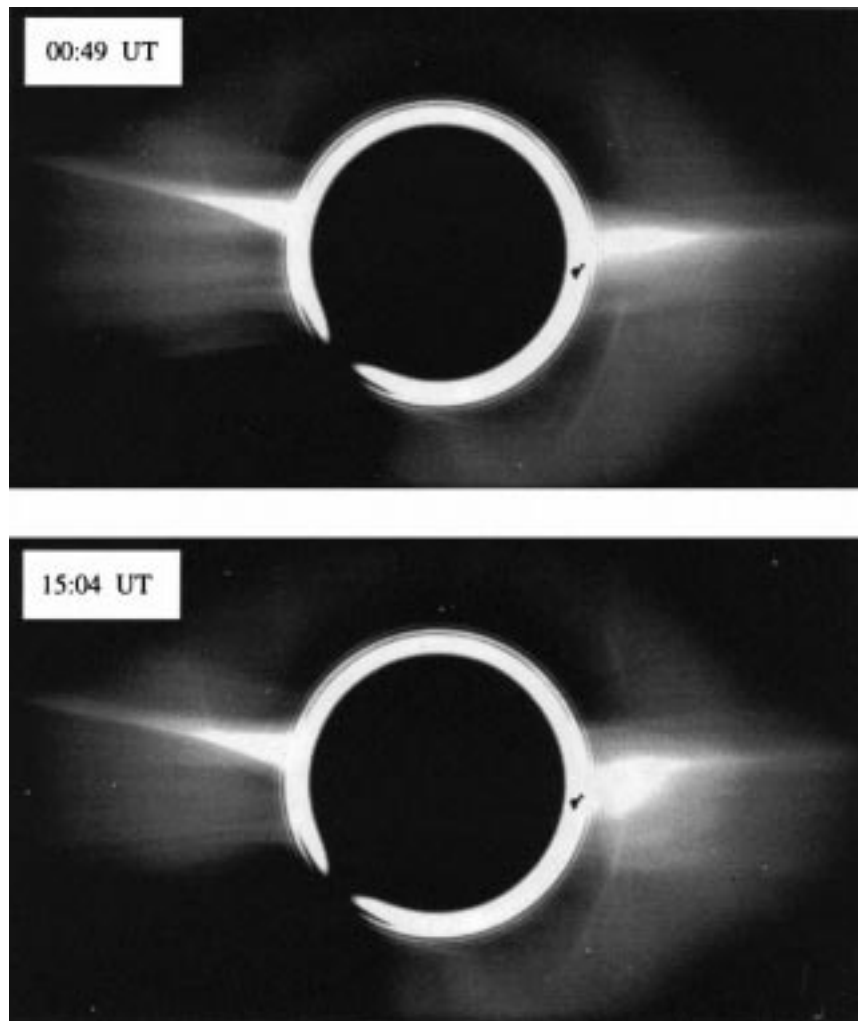
Figure 2. The growth of the streamer on July 28. The images are from the C2 coronagraph, where the diameter of the occulting disc is 1.5 $R_\odot$. The times of the images are in the upper left of each frame. The west limb is to the right and north is at the top on all figures. The image is taken with a clear filter and polarizer. The appeearence of the west equatorial streamer at 00:49 UT was similar to that over the previous 12 hours. The image at 15:04 UT shows not only a significant brightening, but also a marked swelling. Note that the appearance of the east limb is little changed.

stem. In this sequence another, fainter, ejection may be seen moving outwards at a projected angle around 20° south of the equator.

Unfortunately LASCO suffered a data gap between 06:06 and 14:00 UT, so when the event is next seen it has a rather different appearance, as may be seen in Figure 5. These are again differenced C3 images, so the very dark radial feature off the west limb is an artefact caused by rotation of the bright streamer between the
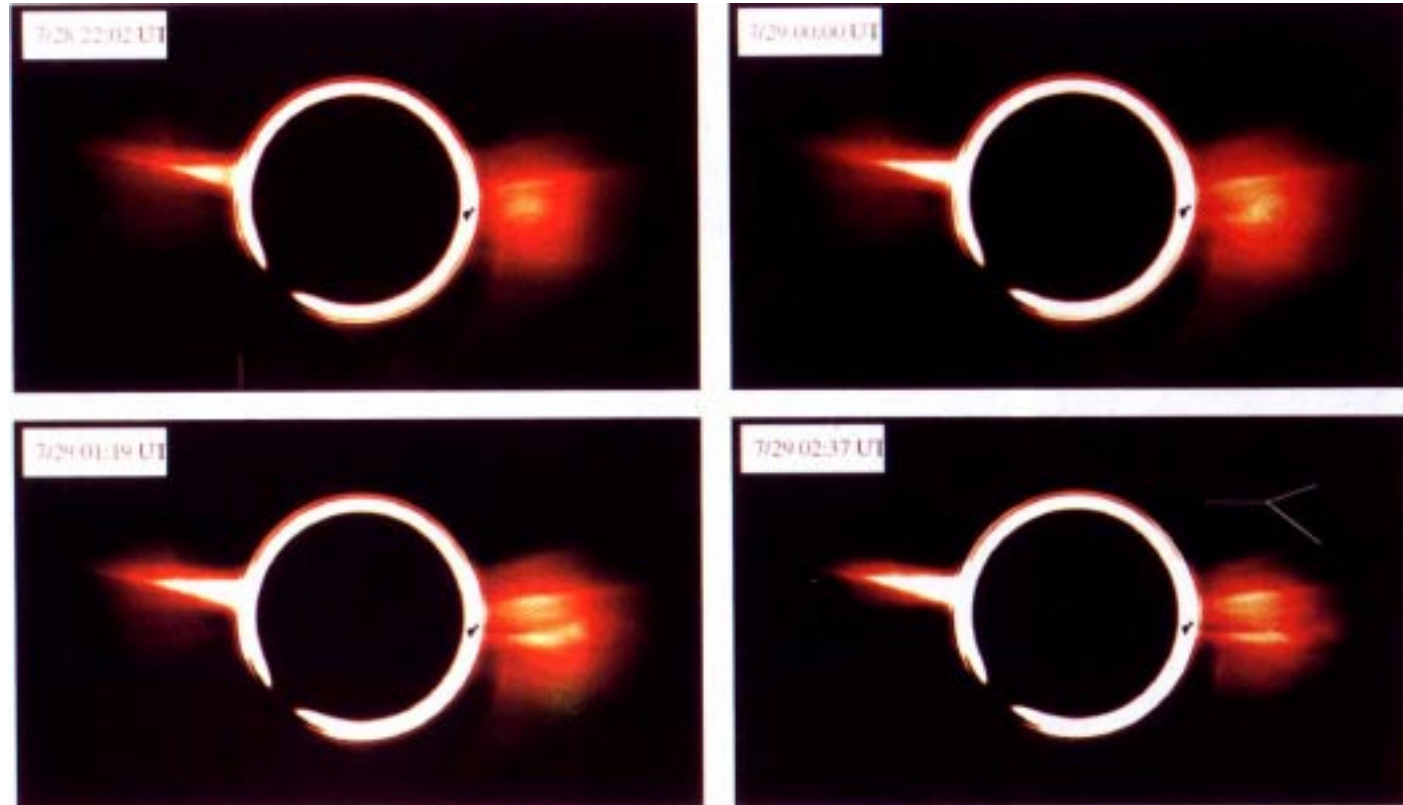
Figure 3. The evolution of the July 28–29 event as seen by the C2 coronagraph. The times of the images are given in the upper left of each frame and the sequence goes from left to right. (July 29, 22:02 UT) This image shows a bright, pear-shaped feature which is embedded within the expanded helmet streamer. (July 29, 00:00 UT and July 29, 01:19 UT) The mass has moved outwards, leaving a bright strip connecting back towards the Sun. (July 29, 02:37 UT) In this image the contrast has been enhanced to highlight the bifurcation of a thin bright sheet slightly to the north of the main ejection. The feature is reproduced in white in the upper part of the frame to aid the eye. The trailing edge of the ejected mass is just visible on the right.

←— 20 solar radii —→
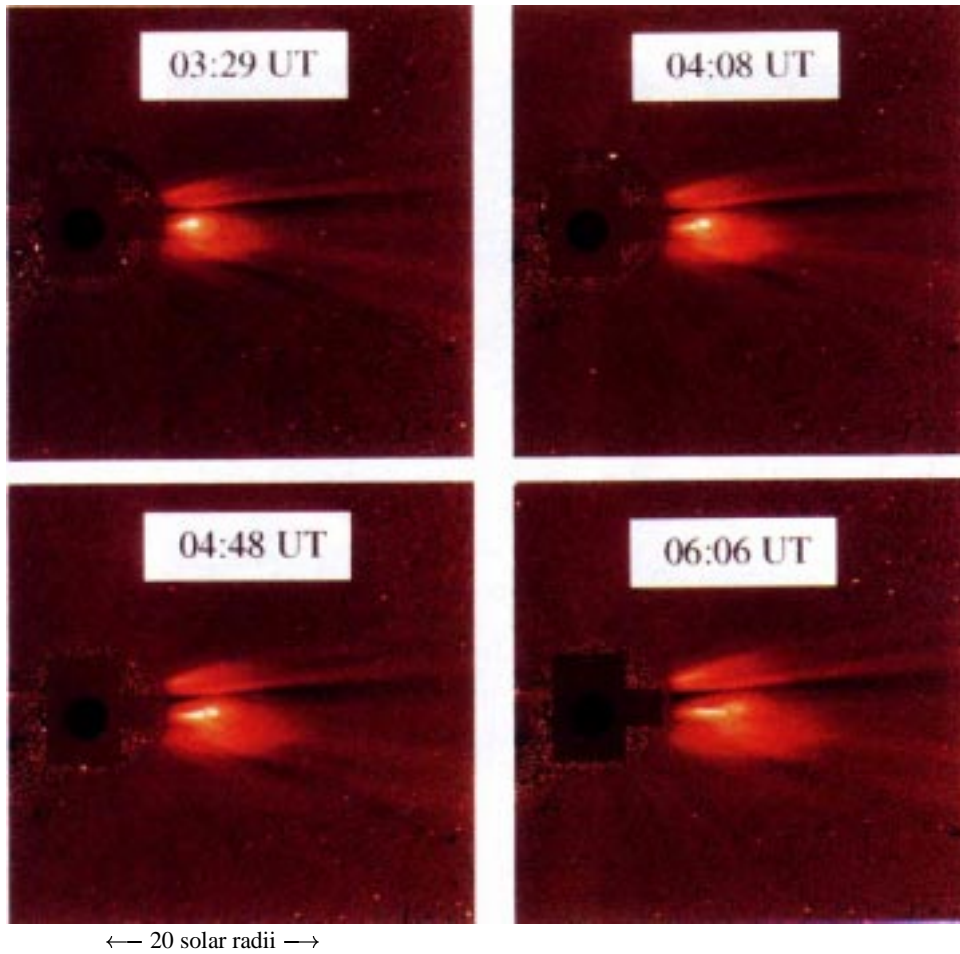
Figure 4. The ejection as seen in the C3 coronagraph, in four images taken at 03:29, 04:08, 04:48, and 06:06 UT, respectively. These images have all had a pre-event image subtracted, and therefore may contain some artefacts caused by rotation of the streamer. The appearance of the transient bright feature is not affected by this. This sequence shows the evolution of the height of the ejected mass with the bright, thin column linking back to the Sun.

image shown and the subtracted image. However, the important feature of these images is the dark '<'-shaped rarefaction which is visible in the centre of the image at 14:00 UT. This feature could be tracked all the way out to the edge of the field of view, although after around 25 $R_\odot$ it became very difficult to identify and could be seen best by viewing a moving sequence of images. The projected angle between the two dark lines in the '<' is 75°. Not only does the rarefaction propagate all the way out to 30 $R_\odot$, but it maintains the same angle throughout.

It has recently been possible to supplement this paper with a CD-ROM movie to illustrate the dynamic phenomena taking place during this mass ejection. The
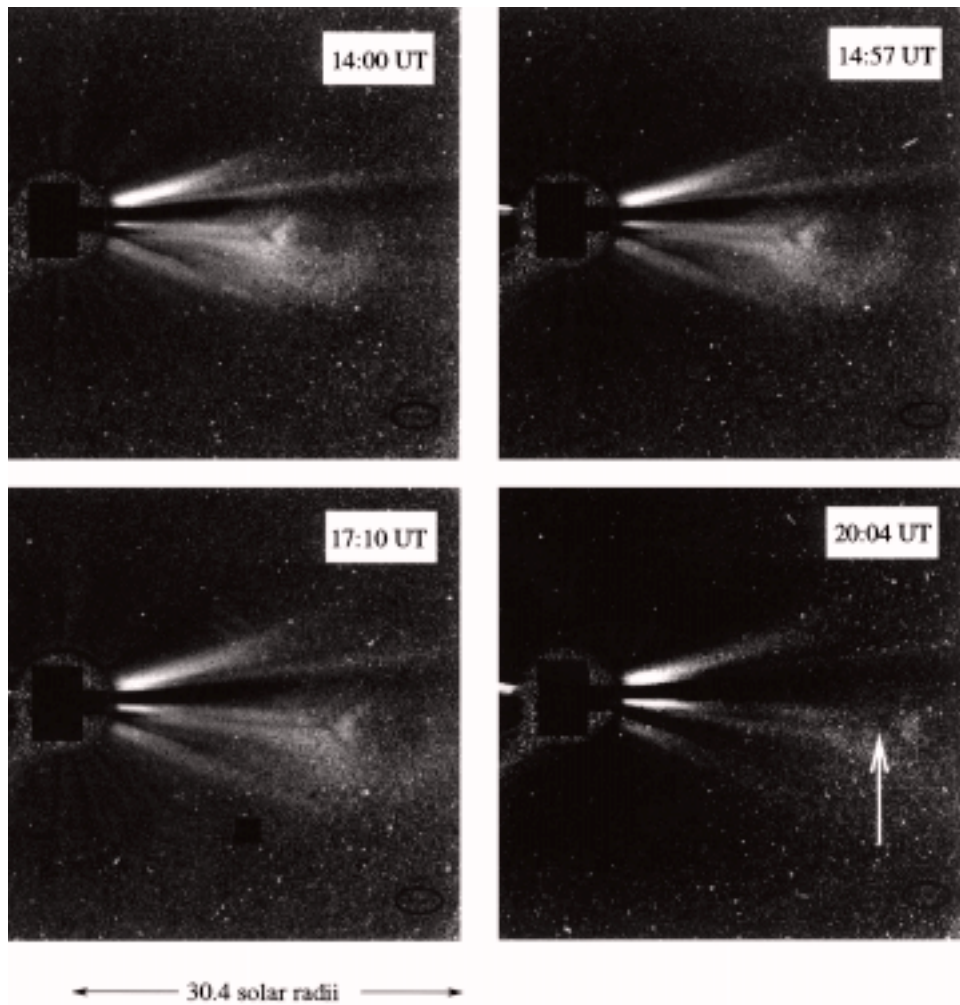
Figure 5. The motion of a '<'-shaped rarefaction which developed behind the ejected mass. It is visible in the centre of the image taken at 14:00 UT on July 29. By 17:10 UT it is still quite clear, but by 20:04 it is becoming difficult to identify. The white arrow points to the apex of the '<' in this last frame. The projected angle, in the plane of the sky, between the two dark lines in the '<' is $75°$.

first movie covers the July 28–29 event, and it is in two parts. The first part shows a composite of the C2 and C3 fields of view. The second part shows just the C2 field of view. The main mass ejection is very clear, and in the frame at 03:17 UT on July 29 the beginning of the '<'-shaped rarefaction behind the main mass ejection can be seen. The second movie shows the C2 field-of-view for November 4 until 06:00 UT on November 6. This is the subject of the second event discussed below. There are two features of interest here. The first is that just prior to the mass ejection off the west limb, there is an event off the east limb. Second, from 19:00 UT on
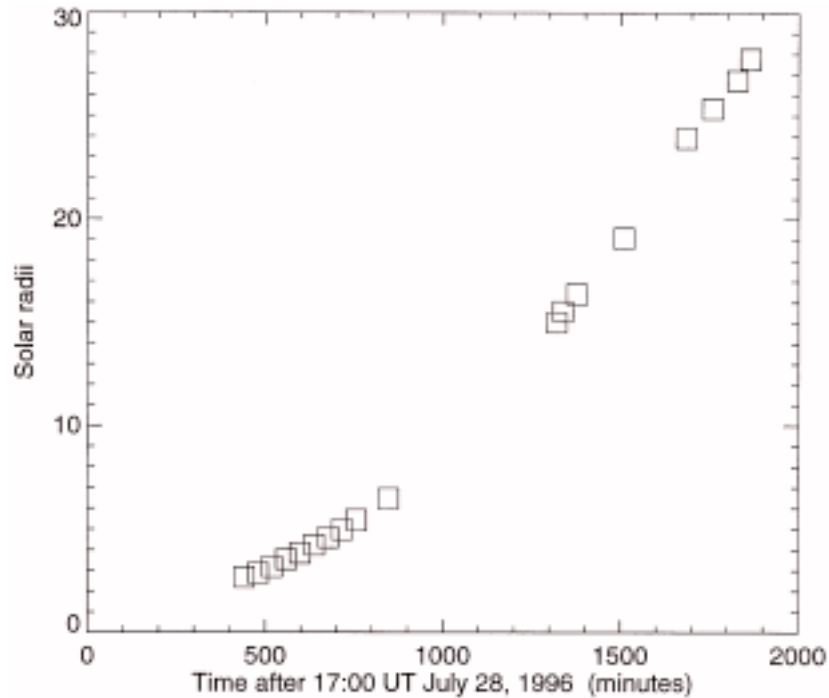
Figure 6. The height – time plot of the apex of the '<', clearly identified in Figure 5. The velocity in the lower part of the plot is 110 ± 5 km s^{-1} and in the outer region it is 269 ± 10 km s^{-1}.

November 5 the bifurcation, which we have argued is a manifestation of a current sheet caused by reconnecting magnetic fields, is clearly visible behind the main mass ejection. The movie representation of the events provides a much better visual impact than the still frames shown in the figures.

The apex of the '<' provides a useful reference for studying the evolution of the velocity of the ejected material. This is shown in Figure 6. Here it is clear that the event has undergone significant acceleration in the vicinity of 5 to 6 $R_\odot$. The velocity before the data gap is not quite constant, as there is a very slight acceleration between 2 and 5 $R_\odot$, but the average projected velocity is 110 ± 5 km s^{-1} In the region above 15 $R_\odot$ the velocity is 269 ± 10 km s^{-1}. It is very clear from Figure 6 that the '<' feature is moving out at a constant velocity, with neither acceleration nor deceleration.

2.2. THE NOVEMBER 5 EVENT

The second event we discuss here occurred on November 5. During this period the LASCO/C1 coronagraph was making occasional line scans with the Fabry– Pérot interferometer in the line of Fe X, and Figure 7 shows an Fe X image taken at 04:30 UT. This image is obtained by dividing the image taken at the center of

Figure 7. The onset of the event at 04:30 UT as seen in the spectral line of Fe X at λ637.4 nm. The image is made by taking an image in the centre of the line and dividing it by the average of the images taken 0.02nm either side of line centre. The diameter of the occulting disc is 1.1 $R_\odot$.

the line, at λ637.4 nm, by the average of images taken 0.02 nm either side of line centre. The bright patch approximately 0.2 $R_\odot$ above the west limb is believed to represent hot material in the corona. Unfortunately there was no further Fe X line scan made that day, so we do not know if this represents the onset of the mass ejection or merely a coronal site where high density/high temperature material is concentrated. However, examination of the remainder of this image shows no other detached coronal feature; only the region off the north-east limb is of comparable brightness, and this is clearly linked down to below the level of the occulting disc (1.1 $R_\odot$). Underneath the bright feature (towards the west limb) there is a hint of a bright arc which is concave outwards. If this is a real feature it is in the correct orientation to be the same structure as is seen later.

By around 10:00 UT there is a mass ejection seen moving above the west limb by the C2 coronagraph. However, the image clearly shows a bubble with a dense (bright) core. Figure 8 (upper frame) shows the C2 image at 12:30 UT, where the dense plasma ball is visible inside a somewhat less dense cloud of gas. Note the sharp boundary to the south of the event in what might be described as the halo
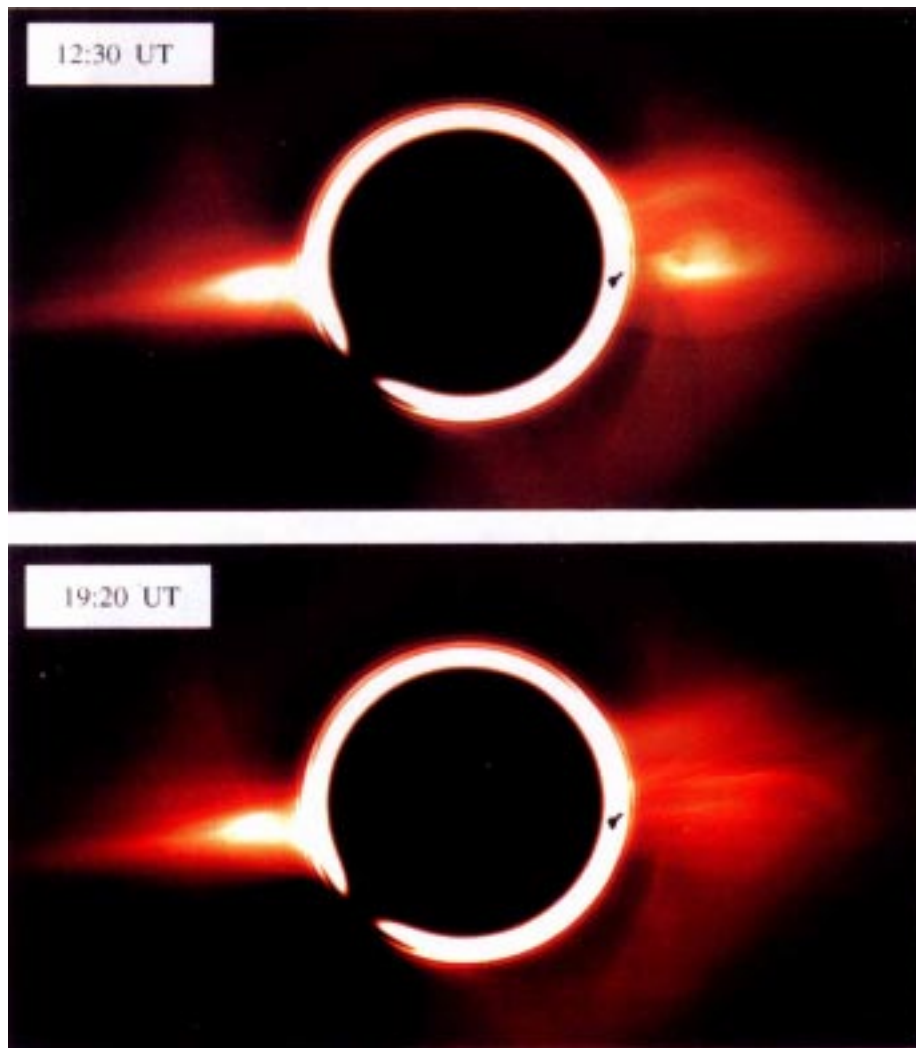
Figure 8. Upper panel: the appearance of the ejected mass at 12:30 UT on November 5. *Lower panel*: the sharp, linear features which were visible behind the ejected mass at 19:30 UT. The one in the center is immediately behind the main mass ejection and shows a bifurcation at around 4 $R_\odot$. There are two similar features at lower projected heights.

surrounding the main ejection; to the north it merges with the pre-existing streamer in this projected image. Figure 8 (lower frame) shows the image at 19:20 UT, when the ejected plasmoid has moved out towards the right edge of the C2 image. Close examination of this image reveals several narrow, bright rays, with bifurcations at increasing radial distance. The most obvious one in Figure 8 is right behind the main ejection, which is actually a double feature. There are two more visible, one almost exactly on the equator and the other about 25° north. These thin density
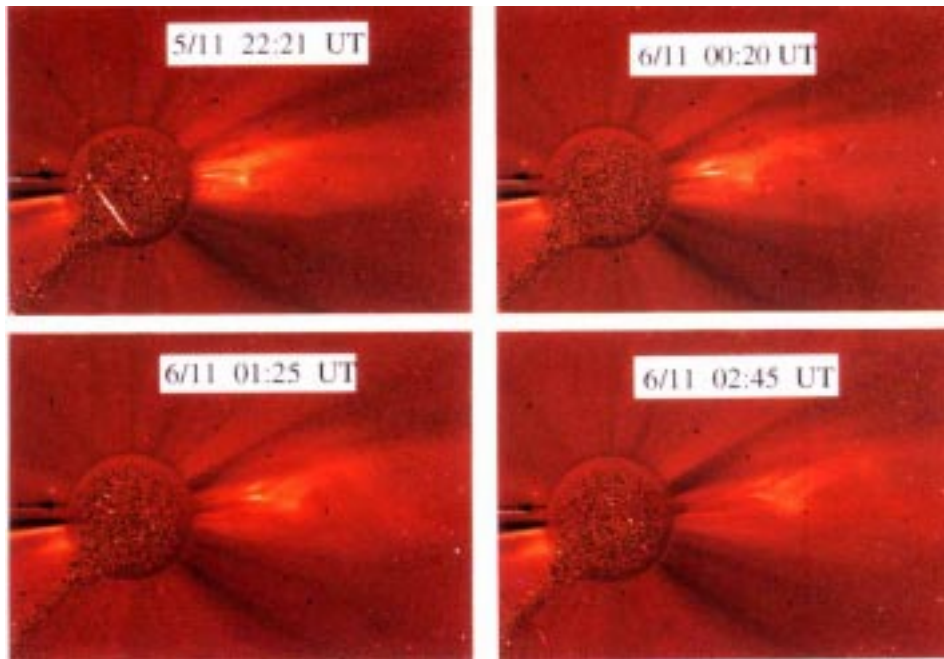
Figure 9. The evolution of the November 5–6 event around the time of the acceleration. The images are from the C3 coronagraph.

enhancements are interpreted as signatures of current sheets formed by magnetic reconnection in the structures associated with the CME; they are visible in the C2 images for several hours, and the 'Y' features move outwards, presumably tracking the main CME.

The CME continued to move outwards through the corona and underwent a significant acceleration around the end of November 5. Figure 9 shows a sequence of four C3 images which illustrate the evolution of the event from 22:21 UT to 02:45 UT (November 6). The image at 00:20 UT (November 6) is particularly interesting as it shows (a) the main bubble with a thin bright straight line linking back to the Sun, but also a second bright line to the north. This line is probably associated with a second ejected bubble which is behind the first bubble as seen from SOHO. Thus a given event may comprise at least two distinct ejected mass bubbles, or plasmoids.

The 'Y' shaped boundary in the bright rays gives the event a distinct feature which may be readily tracked. Figure 10 shows the height-time plot in the plane of the sky for this feature. The points above $10\,R_\odot$ lie on a straight line, corresponding to a projected velocity of $310 \pm 10\ \mathrm{km\ s^{-1}}$. For most of the passage through C2 the velocity is around $54\ \mathrm{km\ s^{-1}}$, although there is some slight acceleration as may be seen by a careful examination of Figure 10. We have plotted the Fe X point from
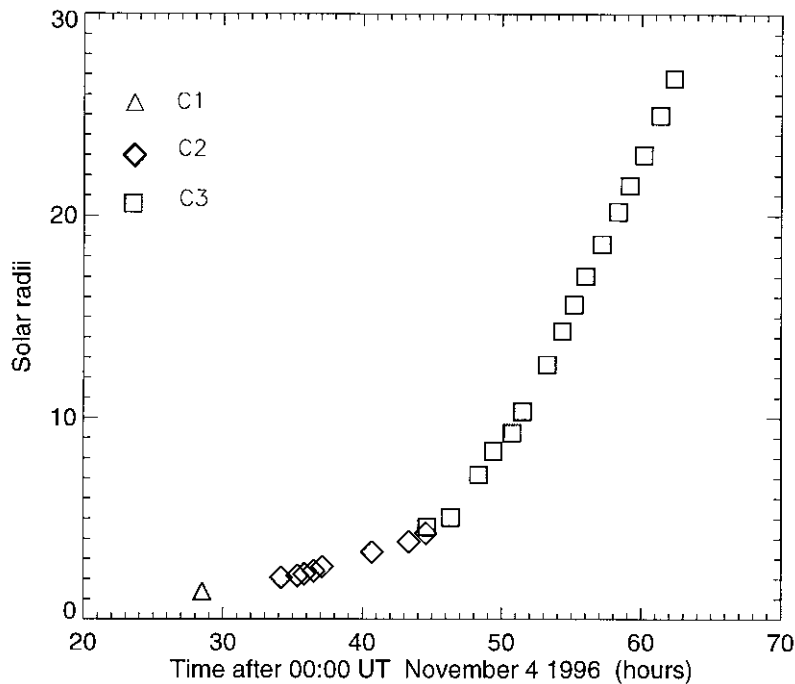
Figure 10. The height-time profile of the trailing edge of the mass ejection for the November 5 event. The different symbols indicate the coronagraph which has imaged the event at the indicated times.

C1 as well, and this falls on a reasonable extrapolation of the C2 points. The main acceleration of the event occurs around 5 $R_\odot$.

3. Discussion

The two events reported here are clear examples of disconnected plasmoids ejected from the Sun. The ejected mass has the appearance of a bubble of dense gas. Comparison of the west limb appearance of the July event (Figure 3, upper panels) with the November event (Figure 8, upper panel) illustrates this well. Moreover, from casual inspection of these images one could be excused for thinking that they were the same event. There have been many attempts to understand the underlying physics of a CME (e.g., Low, 1994). Furthermore, numerical modelling is now advanced to the point that many details for different types of CME can be addressed (e.g., Wang *et al.*, 1995). In fact, Wang *et al.* (1995) have described simulations which have somewhat similar properties to the events discussed here.

An unexpected observation is that of the thin bright rays, with bifurcations at the trailing edge of the ejected plasmoid. The July 28–29 event has one such feature, while the November 5 event has several. We interpret these features as current sheets, similar to those discussed by Petschek (1964). Plasma flows in towards the

boundary layer induce magnetic reconnection, while at the same time matter is ejected outwards along the magnetic field lines. There is enhanced plasma pressure at the centre of the current sheet, which shows up in the C2 images as a bright feature due to a density enhancement. The bifurcation point is then interpreted as the local magnetic reconnection site. The November 5 event shows at least three current sheets which move outwards through the corona at approximately the same speed. This is interpreted as multiple, discrete mass ejections in the same general direction. If they were at widely separated longitudes, then we would expect the projected images to show some velocity dispersion. We believe this is an important facet of this event which should be taken into account by the modellers.

The other interesting feature of the July 28−29 event is the 'V'-shaped rarefaction which is visible moving out through the corona to beyond the edge of the field of view at ∼30 $R_{\odot}$. This rarefaction is already visible in some of the C2 images (not shown), so it forms relatively close to the Sun, and is probably a manifestation of a cavity in the magnetic field such as is shown in Figure 1. We believe that the observations of this feature are partly a fortuitous result of a favourable viewing angle, as the rarefaction we have identified must clearly be a three-dimensional structure. Thus if it were viewed at a different angle, it would certainly look very different, and probably would not be visible at all. Thus for this event, the velocity of the ejecta was probably very close to $90°$ to the line of sight, in which case the projected velocity of 269 km s^{-1} must be very close to the actual velocity.

The acceleration of the plasmoids in the region of 5−6 $R_{\odot}$ we believe is an indication of where they get accelerated by the solar wind, such that they then move outwards into the interplanetary medium at the solar wind velocity. The velocity of both ejecta in the region beyond 10 $R_{\odot}$ is consistent with the velocity of the slow solar wind, when projection effects are taken into account. Furthermore, this general acceleration profile may well represent the acceleration profile of the slow solar wind. In this case, the source surface at low latitudes of the solar wind would be around 6 $R_{\odot}$. If this were not to be the case, then some other agent must be invoked for accelerating the plasmoids at this radial distance.

It is evident from the behaviour of the equatorial streamer on July 28 that prior to the mass ejection there had been a steady input of mass to the corona. This was responsible for the streamer swelling shown in Figure 2. The triggering of the CME is presumably a result of increased pressure within the magnetic field in or adjacent to the streamer. The pressure increase can be due to enhanced density, increased temperature, or most likely a combination of both. The C2 coronagraph responds to light scattered off free electrons and therefore any increase in brightness, such as that shown in Figure 2, is caused by increased mass along the line of sight. Virtually the only source of this mass is the chromosphere and it is presumably the result of gentle evaporation.

If our interpretation of the bright rays visible in Figures 3 and 8 as current sheets is correct, the magnetic reconnection that leads to the current sheets will also accelerate charged particles. Coulomb losses of these particles will increase

the gas temperature within the swelling structure, thus increasing the tendency towards instability (Simnett and Harrison, 1985).

Acknowledgements

References

Brueckner, G. E. and 14 co-authors: 1995, *Solar Phys.* **162**, 357.

Illing, R. M. E. and Hundhausen, A. J. : 1983, *J. Geophys. Res.* **88**, 10 210.

Low, B. C.: 1994, *Proceedings of the Third SOHO Workshop 'Solar Dynamic Phenomena and Solar Wind Consequences'*, ESA SP-373, p. 123.

Low, B. C.: 1996, *Solar Phys.* **167**, 217.

McComas, D. J., Gosling, J. T., Phillips, J. L., Bame, S. J., Luhmann, J. G., and Smith, E. J.: 1989, *J. Geophys. Res.* **94**, 6907.

McComas, D. J., Phillips, J. L., Hundhausen, A. J., and Burkepile, J. T.: 1991, *Geophys. Res. Letters* **18**, 73.

Petschek, H. E.: 1964, *The Physics of Solar Flares*, NASA SP-50, p. 425.

St. Cyr, O. C. and Burkepile, J. T.: 1990, NCAR Technical Report, NCAR TN-352+STR.

Simnett, G. M. and Harrison, R. A.: 1985, *Solar Phys.* **99**, 291.

Wang, A. H., Wu, S. T., Suess, S. T., and Poletto, G.: 1995, *Solar Phys.* **161**, 365.

Webb, D. F. and Cliver, E. W. : 1995, *J. Geophys. Res.* **100**, 5853.